BiPOLES: a tool for bidirectional dual-color optogenetic control of neurons

Johannes Vierock[2]*, Silvia Rodriguez-Rozada[1]*, Florian Pieper[3], Alexander Dieter[1], Amelie Bergs[4], Nadja Zeitzschel[4], Joachim Ahlbeck[3], Kathrin Sauter[1], Alexander Gottschalk[4], Andreas K. Engel[3], Peter Hegemann[2], J. Simon Wiegert[1+]

[1]Institute for Biology, Experimental Biophysics, Humboldt University Berlin, D-10115 Berlin Germany

[2]Research Group Synaptic Wiring and Information Processing, Center for Molecular Neurobiology Hamburg, University Medical Center Hamburg-Eppendorf, 20251 Hamburg, Germany

[3]Department of Neurophysiology and Pathophysiology, University Medical Center Hamburg-Eppendorf, 20246 Hamburg, Germany

[4]Buchmann Institute for Molecular Life Sciences and Institute of Biophysical Chemistry, Goethe University, Max-von-Laue-Strasse 15, 60438 Frankfurt, Germany

*equal contribution

+correspondence to: simon.wiegert@zmnh.uni-hamburg.de

Abstract

We report BiPOLES, an optogenetic tool for balanced excitation and inhibition of neurons with light of two different colors. BiPOLES consists of the blue-light-sensitive anion-conducting channelrhodopsin *Gt*ACR2 fused to the red-light-sensitive cation-conducting channelrhodopsin Chrimson in a single, trafficking-optimized tandem protein. BiPOLES enables multiple applications including potent dual-color spiking and silencing of the same neurons *in vivo* and dual-color optogenetic control of two independent neuronal populations.

Main text

To prove necessity and sufficiency of a particular neuronal population for a specific behavior, a cognitive task, or a pathological condition, it is desirable to both faithfully inhibit and activate this exact same population of neurons. In principle, optogenetic manipulations should allow such interventions. However, excitation and inhibition of the neuronal population of interest is commonly done in separate experiments, expressing either an excitatory or an inhibitory opsin. Alternatively, if both opsins are co-expressed in the same cells, it is essential to achieve equal subcellular distribution and a defined ratio between excitatory and inhibitory action at the respective wavelengths, so that neuronal activation and silencing can be precisely controlled in all transduced cells. This is particularly challenging when AAV-transduction of the optogenetic actuators is required *in vivo*.

A second, long-standing challenge in neuroscience is the independent activation of two defined neuronal populations. Although two spectrally distinct opsins have been combined previously to spike two distinct sets of neurons[1-4], careful calibration and dosing of blue light is required to avoid activation of the red-shifted opsin, as all rhodopsins are activated to a certain extent by blue light. This typically leaves only a narrow spectral and energetic window to activate the blue- but not the red-light-sensitive opsin. Thus, dual-color control of neurons is particularly challenging in the mammalian brain where light intensities decrease by orders of magnitude over a few millimeters in a wavelength-dependent manner[5,6].

Capitalizing on the recent advent of anion-conducting channelrhodopsins (ACRs)[7-9] and a tandem gene-fusion strategy[10], we generated BiPOLES, a Bidirectional Pair of Opsins for Light-induced Excitation and Silencing. First, BiPOLES enables potent, light-mediated silencing and activation of the same neurons *in vivo* by a single optogenetic tool and second, dual-color control of two distinct neuronal populations without cross-talk at light intensities spanning multiple orders of magnitude, when combined with a second blue-light-sensitive Channelrhodopsin (ChR).

As a general strategy, we fused the red-light-activated cation channel Chrimson with various blue- or green-light-activated ACRs. This approach aimed for colocalized and balanced hyper- and depolarization with blue and red light starting from a physiological membrane voltage as well as restriction of the depolarizing light spectrum to a narrow, orange-red window as the ACR compensates the blue-light-activated Chrimson currents. The opsins were linked by sequences composed of the Kir2.1 membrane trafficking signal (ts)[11], a cyan or yellow fluorescent protein, and the transmembrane β helix of the rat gastric H^+/K^+ ATPase (βHK) to maintain correct membrane topology of both opsins[10] (Fig. 1A).

All ACR-Chrimson tandems were evaluated in human embryonic kidney cells (HEK) under matched experimental conditions. In all constructs, except the one lacking the βHK-subunit, blue-light-activated currents shifted towards the chloride Nernst potential whereas red-light-activated currents shifted towards the proton Nernst potential (Fig.1B-D, S1). Reversal potentials varied strongly for the different tandem variants indicating considerable differences in the wavelength-specific anion/cation conductance ratio (Fig.1D). At a defined membrane potential between the Nernst potential for chloride or protons, blue and red light induced outward and inward currents, respectively. The specific wavelength of photocurrent inversion (λ_{rev}) depended on the action spectrum of the ACR, the relative conductance of the ACR and Chrimson, and the relative driving force for anions, cations and protons defined by the membrane voltage and the respective ion gradients (Fig.1E).

*Gt*ACR2-ts-mCerulean-βHK-Chrimson – from here on termed BiPOLES – was the most promising variant, showing first, the largest difference in reversal potential upon blue- or red-light excitation (Fig.1D), second, equal inward and outward currents at -60 mV, which is near the resting membrane voltage (Fig.1E) and, third, the highest red-light-activated photocurrents, comparable to those of Chrimson expressed alone (Fig.1F).

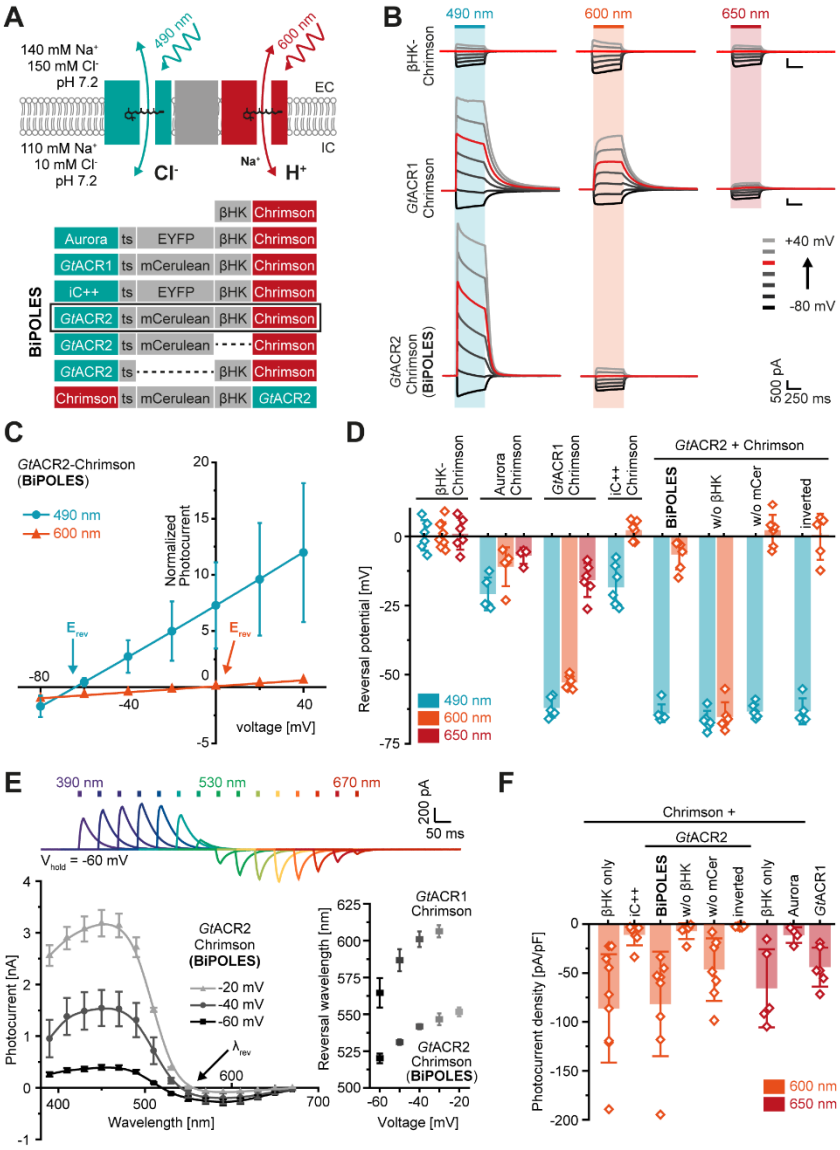

Figure 1: Development of BiPOLES and biophysical characterization. (A) Molecular scheme of BiPOLES with the extracellular (EC) and intracellular (IC) ionic conditions used for HEK293-cell recordings. The blue-green-light-activated natural anion channels *Gt*ACR1 and *Gt*ACR2 or the engineered ChR-chimeras iC++ and Aurora were fused to the red-light-activated cation-conducting Chrimson by a transmembrane spanning linker region consisting of a trafficking signal (ts), a yellow or cyan fluorescent protein (EYFP, mCerulean3) and the βHK transmembrane fragment. The fusion construct termed BiPOLES is indicated by a black frame. **(B)** Representative photocurrents of βHK-Chrimson-mCerulean (top), *Gt*ACR1-ts-mCerulean-βHK-Chrimson (middle) *Gt*ACR2-ts-mCerulean-βHK-Chrimson (BiPOLES, bottom) in whole-cell patch clamp recordings from HEK293 cells at 490, 600 and 650 nm illumination. **(C)** Normalized peak photocurrents of BiPOLES at different membrane

voltages evoked at either 490 or 600 nm (see panel B, mean ± SD; n = 6 - 8; normalized to the peak photocurrent at -80 mV and 600 nm illumination). **(D)** Reversal potential of early peak photocurrents during 500-ms illumination with 490, 600, or 650 nm light as shown in (B) (mean ± SD; n = 5 - 8). **(E)** Top: Representative photocurrents of BiPOLES with 10 ms light pulses of different color and equal photon flux at -60 mV. Lower left: Action spectra of BiPOLES at different membrane voltages (λ_{rev} = photocurrent reversal wavelength, mean ± SEM, n = 4 - 9). Lower right: λ_{rev} of *Gt*ACR1-ts-mCerulean-βHK-Chrimson and BiPOLES at different membrane voltages (mean ± SD; n = 3 - 9). **(F)** Peak photocurrent densities at -80 mV and 600 nm or 650 nm illumination as shown in (B) (Mean ± SD; n = 5 - 8).

Next, we validated the bidirectional action and the applicability of BiPOLES as an optogenetic tool in CA1 pyramidal neurons of rat hippocampal slice cultures. We observed membrane-localized BiPOLES expression, most strongly in the somatodendritic compartment (Fig. 2A). Illumination triggered large photocurrents with biophysical properties similar to those observed in HEK cells (Fig. S2). To enhance membrane trafficking and to avoid axonal localization of BiPOLES, we generated a soma-targeted variant (somBiPOLES) by attaching a C-terminal Kv2.1-trafficking sequence[12]. somBiPOLES showed improved membrane localization (Fig. 2A, S9A), enhanced photocurrents (Fig. S3) and higher light sensitivity compared to BiPOLES (Fig. S4). In current-clamp recordings orange and red light reliably induced action potentials (APs) in somBiPOLES expressing cells with a similar efficacy as Chrimson (Fig. 2B, S4). Notably, blue light up to 100 mW/mm^2 did not trigger APs due to robust shunting by *Gt*ACR2, whereas Chrimson alone induced spikes also with blue light above 0.95 mW/mm^2 (Fig. 2B, S4). Next, we tested the silencing capabilities of BiPOLES and somBiPOLES by measuring their ability to shift the rheobase (see Methods) and suppress APs with blue light. Both variants significantly shifted the rheobase towards larger currents at intensities above 0.1 mW/mm^2 (Fig. 2C, S5), with somBiPOLES showing complete spike block in some cases. We further demonstrate the potent silencing capacity of somBiPOLES and BiPOLES by combining blue- and red-light pulses showing that red-light-evoked spikes were reliably inhibited with a coinciding blue-light pulse (Fig. 2D). Moreover, simultaneous illumination with blue and orange light at varying ratios enabled dynamic clamping of the neuronal membrane voltage (Fig. S6). Taken together, BiPOLES and somBiPOLES enable efficient, bidirectional control of neuronal activity.

Since BiPOLES permits neuronal spiking exclusively with orange-red light, this opens new possibilities for two-color excitation of genetically distinct but spatially intermingled neuronal populations using a second, blue-light-activated ChR. To demonstrate this, we expressed somBiPOLES in CA1 VIP interneurons and CheRiff, a blue-sensitive ChR (λ_{max} = 460nm)[13] in CA1 pyramidal neurons (Fig. 2E, see Methods for details). CheRiff-expressing pyramidal cells

were readily spiking upon blue, but not orange-red illumination up to 10 mW/mm^2 (Fig. 2E, S4). Conversely, red but not blue light triggered APs in somBiPOLES-expressing VIP neurons (Fig. 2E). Next, we recorded synaptic inputs from these two populations onto VIP-negative GABAergic neurons in stratum-oriens (Fig. 2F). As expected, blue light triggered EPSCs (CheRiff) and red light IPSCs (somBiPOLES), evident by their respective reversal potentials at 8.8 ± 10.4 mV and -71.4 ± 13.1 mV (Fig. 2F).

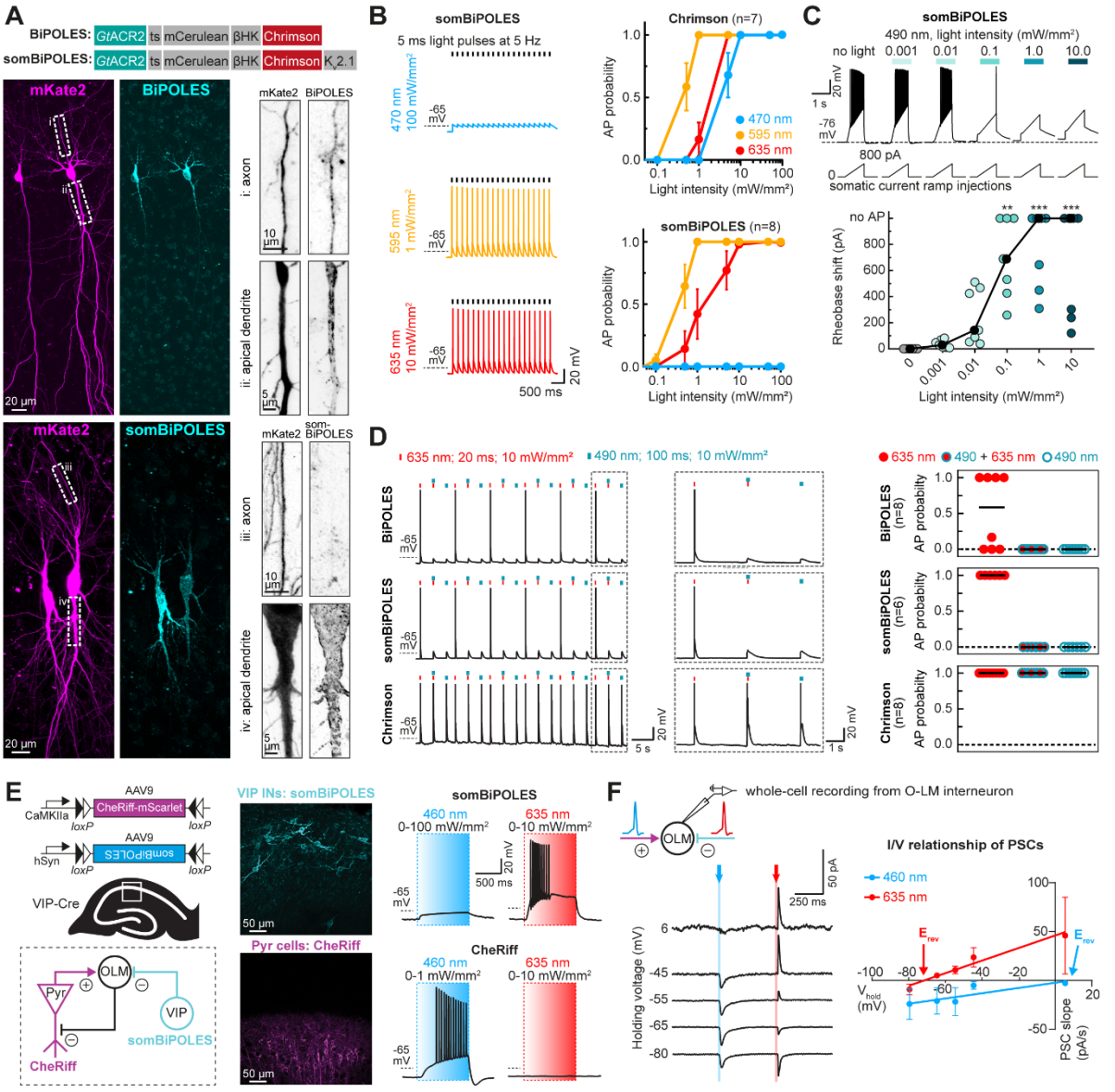

Figure 2: Excitation and silencing of hippocampal neurons with BiPOLES and somBiPOLES. (A) Molecular scheme of BiPOLES and somBiPOLES as used in neurons and maximum-intensity projection images of 2-photon stacks showing expression of BiPOLES (top) or soma-targeted BiPOLES (somBiPOLES, bottom) co-expressed with mKate2 in CA1 or CA3 pyramidal neurons of organotypic hippocampal slices. Magnified views of axonal or somato-dendritic compartments are shown as inverted gray-scale images. Note absence of somBiPOLES in the axon. **(B)** Current-clamp (IC) characterization of somBiPOLES and Chrimson in CA1 pyramidal cells to determine light-evoked action potential (AP)-

probability at different wavelengths. Left: Example traces. Right: quantification of light-mediated AP probability at indicated wavelengths and intensities (mean ± SEM, n = 7 - 8). **(C)** IC characterization of somBiPOLES-mediated neuronal silencing. Current ramps (from 0–100 to 0–900 pA) were injected into somBiPOLES-expressing CA1 pyramidal cells to induce APs during illumination with blue light at indicated intensities (from 0.001 to 10 mW/mm^2, black circles: medians, n = 7, Friedman test, **p < 0.01, ***p < 0.001). **(D)** IC characterization of bidirectional optical spiking-control with BiPOLES and somBiPOLES. Left: Voltage traces showing red-light-evoked APs, which were blocked by a concomitant blue light pulse in (som)BiPOLES expressing cells. Right: quantification of AP probability under indicated conditions (black horizontal lines: medians, n = 6 - 8). **(E)** Independent dual-color control of two neuronal populations with somBiPOLES and CheRiff. Left: strategy to achieve mutually exclusive expression of CheRiff-mScarlet in CA1 pyramidal neurons and somBiPOLES in VIP-positive GABAergic neurons. Both cell types innervate O-LM interneurons in CA1. Middle: Maximum-intensity projection images of 2-photon stacks showing expression of somBiPOLES in VIP-interneurons (cyan) and CheRiff-mScarlet in the pyramidal layer of CA1 (magenta). Right: IC-recordings demonstrating mutually exclusive spiking of somBiPOLES- and CheRiff-expressing neurons under red or blue illumination (see fig. S4 for details). **(F)** Postsynaptic whole-cell voltage-clamp recordings at indicated membrane voltages showing EPSCs and IPSCs upon blue- and red-light pulses, respectively. Right: quantification of blue- and red-light-evoked PSCs and their reversal potential (mean ± SEM, n = 7 - 8).

Next, we used BiPOLES to control cholinergic motor neurons in *C. elegans*. BiPOLES-linked mCerulean was visible at the nerve ring in the head part indicating correct expression and localization of the tool (Fig. 3A). Illumination with red light resulted in body-wall muscle contraction and effective body-shrinkage, consistent with motor neuron activation. Conversely, blue light triggered body extension, indicative of muscle relaxation and thus, cholinergic motor neuron inhibition (Fig. 3B). Maximal body length changes of +3% at 480 nm and -10% at 560-600 nm and reversal of the effect between 480-520 nm were consistent with the inhibitory and excitatory action spectrum of BiPOLES (Fig. 1E, 3B, S7) The light effects on body length required functional BiPOLES as light did not affect body length in the absence of all-*trans* retinal (ATR, Fig. 3B).

To extend the applications of BiPOLES, we generated various conditional and non-conditional viral vectors, in which the expression of the tandem protein is regulated by different promoters (see Methods, Figs. S8-9). Conditionally expressed in noradrenergic neurons of the Locus Coeruleus (LC) in mice, orange illumination of somBiPOLES reliably triggered pupil dilation, indicative of LC-mediated arousal[14] (Fig. 3C-E, S10). Light-mediated pupil dilation was reverted immediately by additional blue light during the orange-light stimulation or suppressed altogether, when blue-light delivery started before orange-light application (Fig. 3D,E), suggesting that orange-light-induced spiking of noradrenergic neurons in LC was efficiently shunted. Thus, LC-neurons were bidirectionally controlled with somBiPOLES.

We hypothesized that targeting BiPOLES to GABAergic neurons enables bidirectional control of excitation/inhibition (E/I) balance. Thus, we generated a viral vector using the minimal *Dlx*

178 promoter [15] (mDlx), verified mDlx-BiPOLES functionality *in vitro* (Fig. S8) and expressed it in
179 GABAergic neurons in ferret secondary visual cortex to modulate E/I-balance during sensory
180 processing (Fig. 3F).

181 Intracortical data obtained from linear probes and under isoflurane anesthesia provided
182 evidence for modulation of cortical activity by shifts in E/I balance (Fig. 3G,H). Blue light led to
183 an increase in baseline activity, consistent with deactivation of inhibitory neurons (Fig. 3G,H).
184 Activation of GABAergic cells by red light did not further decrease the low cortical baseline
185 activity, but significantly reduced cortical responses triggered by sensory stimuli (Fig. 3G,H).
186 Although activating effects of blue light on evoked spiking were not significant in the average
187 data, we obtained clear evidence in individual recordings that blue light could enhance late
188 response components (Fig. 3G), confirming a disinhibitory effect. Overall, these data suggest
189 that BiPOLES is efficient in bidirectional control of inhibitory mechanisms, demonstrating its
190 applicability for the control of E/I shifts in the cortical microcircuit *in vivo*.

191

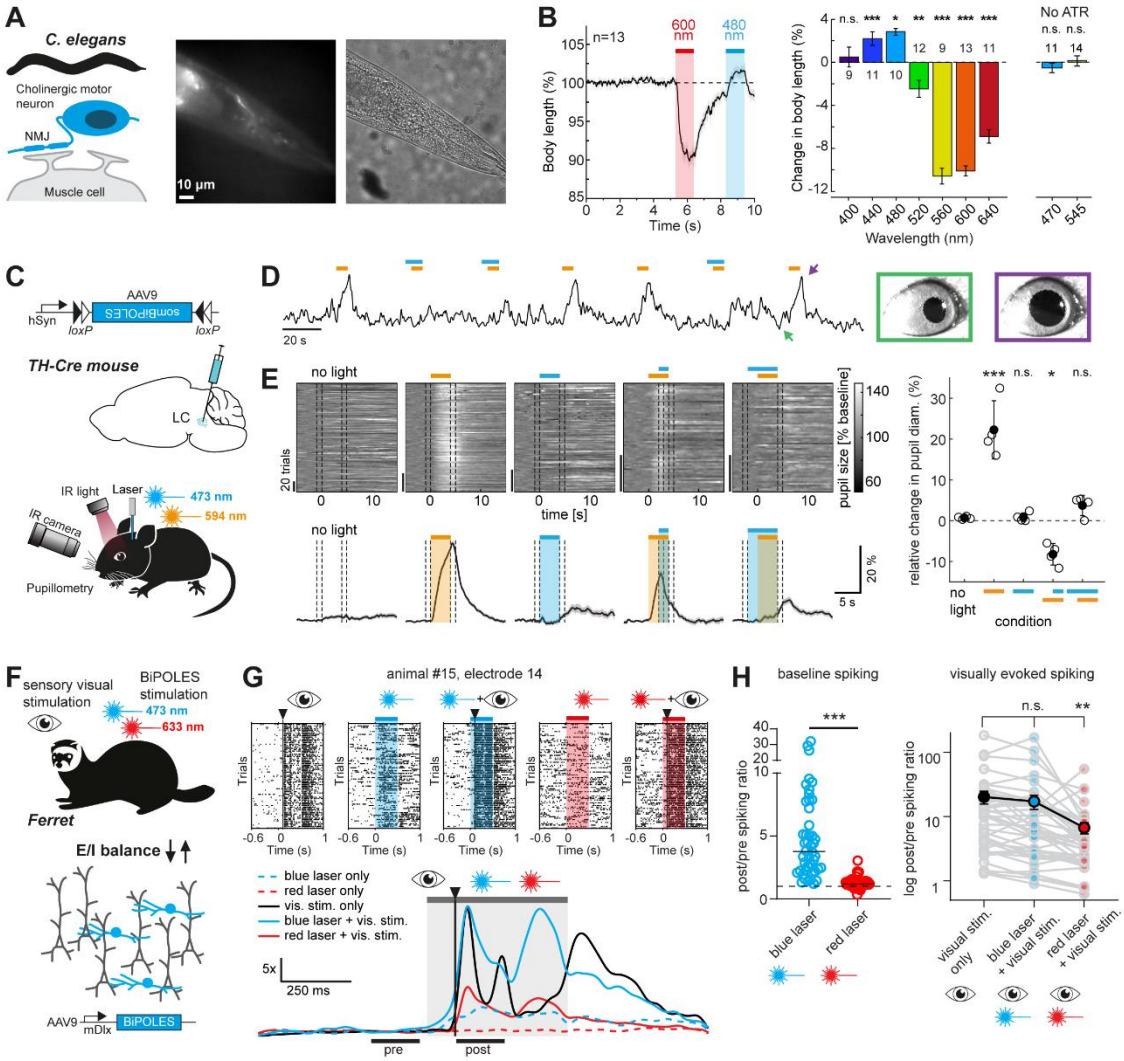

Figure 3: BiPOLES and somBiPOLES allow bidirectional modulation of neuronal activity *in vivo*.

(A) BIPOLES expressed in cholinergic neurons of *C. elegans* enables bidirectional control of body contraction and relaxation. Left: Scheme of BiPOLES-expressing cholinergic motor neuron innervating a muscle cell. Right: Fluorescence and phase contrast micrographs showing expression of BiPOLES in the nerve ring. **(B)** Left: Temporal dynamics of relative changes in body length upon illumination with 600 and 480 nm light (1.1 mW/mm^2, n = 13). Right: Spectral quantification of maximal change in body length (mean ± SEM, n = 9 -14, *p < 0.05, **p < 0.01, ***p < 0.001). **(C)** Conditional expression of somBiPOLES in noradrenergic neurons of the mouse LC to modulate pupil dilation. **(D)** Relative pupil diameter in a single recording session. Orange and blue bars indicate time of illumination with 594 (orange) and 473 nm (blue), respectively. Arrows indicate positions of the two example images of the eye. **(E)** Quantification of normalized pupil size in one animal under various stimulation conditions for somBiPOLES as indicated. Top left: single trials. Bottom left: mean ± SEM. Dashed lines show regions used for quantification in the plot on the right. Right: quantification of relative pupil size (n = 4 mice, *p < 0.05, ***: p < 0.001). **(F)** Modulation of GABAergic neurons (blue) in ferret secondary visual cortex (area 18) with mDlx-BiPOLES. Red (633 nm) or blue (473 nm) laser light was used to (de-)activate interneurons with or without a preceding 10-ms visual flash (LED) to the ferret's right eye. **(G)** Example neuronal spiking responses at one contact of the linear probe (~900 µm depth) under indicated stimulation conditions Top: Raster-plots of the visual stimulus alone, blue laser (+visual), red laser (+visual) conditions. Bottom: Normalized to 'pre'-phase averaged spike-density plot (sigma = 20 ms) of

each indicated condition. Gray area: laser-on epoch; black vertical line: visual stimulus onset. Black horizontal lines indicate the 200 ms pre- and post-stim analysis epochs to compute the results in (H). Note the rate-increase after the onset of the blue laser before the onset of the visual stimulus and the reduced answer after red laser illumination. **(H)** Spike-rate ratio of pos-t vs pre-laser-stimulus epoch. Left: quantification of laser-mediated impact on baseline spiking rate (no visual stim.). Right: quantification of the spike-rate change of the same units during only visual and laser+visual stimulation. (n = 46 contacts showing visual responses from 3 animals, **p < 0.01, ***p < 0.001).

In conclusion, BiPOLES is a tandem of a cation- and an anion-selective ChR that serves as a new optogenetic tool for balanced excitation and inhibition of the same neurons with red and blue light, respectively. Unlike strategies based on an internal ribosomal entry site[16] or self-cleaving viral 2A peptide bridges[17], BiPOLES displays a fixed 1:1 stoichiometry and colocalization of excitatory and inhibitory currents, featuring several advantages. First, it allows for optically clamping the membrane voltage with a defined ratio of red/blue light. Second, since BiPOLES-expressing cells are not excitable with blue light of any intensity, scale-free and independent spiking of two neuronal populations is possible in combination with a second, blue-light-sensitive ChR. Third, BiPOLES can be used to spike or inhibit the same population of neurons *in vivo*, which allows addressing a number of previously inaccessible questions. For example, during extracellular recordings, BiPOLES may be useful for optogenetic identification (optotagging) with red light[18] and optogenetic silencing of the same neurons. Aside from bidirectional control of motor neurons, noradrenergic signaling in LC and GABAergic activity in neocortex, as demonstrated in this study, additional applications for BiPOLES could be bidirectional control of engram neurons[19] to test both necessity and sufficiency of a particular set of neurons for memory retrieval or switching the valence of a particular experience by inhibiting or activating the same or even two distinct populations of neuromodulatory neurons.

Acknowledgements

We thank Stefan Schillemeit, Sandra Augustin and Tharsana Tharmalingam for excellent technical assistance, Mathew McGinley and Peter Murphy for help with pupil analysis, Sonja Kleinlogel for providing plasmids carrying the original opsin tandem cassette and Jonas Wietek for providing ACR plasmids and highly appreciated discussions at an early phase of the project. Ingke Braren of the UKE Vector Facility produced AAV vectors. This work was supported by the German Research Foundation, DFG (SPP1926, FOR2419/P6, SFB963/B8 to J.S.W., SFB936/A2 and SPP2041/EN533/15-1 to A.K.E., SPP1926 to P.H., SFB807/P11 to A.B. & A.G.) and the European Research Council (ERC2016-StG-714762 to J.S.W., Stardust to P.H.). Peter Hegemann is a Hertie Professor and supported by the Hertie Foundation.

Author contributions

Conceptualization, J.V., S.R.R., P.H., J.S.W.; Methodology J.V., S.R.R., F.P., A.D., J.A., A.K.E., A.G., P.H., J.S.W.; Experimentation, J.V., S.R.R., F.P., A.D., A.B. N.Z., J.A.; Analysis, J.V., S.R.R., F.P., A.D., A.B. N.Z., J.A.; Writing, J.V., S.R.R., A.K.E., A.G., J.S.W.; Supervision, A.K.E., A.G., P.H., J.S.W.; Funding Acquisition, A.B., A.K.E., A.G., P.H., J.S.W.

References

1 Klapoetke, N. C. *et al.* Independent optical excitation of distinct neural populations. *Nat Methods* **11**, 338-346, doi:10.1038/nmeth.2836 (2014).

2 Yizhar, O. *et al.* Neocortical excitation/inhibition balance in information processing and social dysfunction. *Nature* **477**, 171-178, doi:10.1038/nature10360 (2011).

3 Akerboom, J. *et al.* Genetically encoded calcium indicators for multi-color neural activity imaging and combination with optogenetics. *Front Mol Neurosci* **6**, 2, doi:10.3389/fnmol.2013.00002 (2013).

4 Erbguth, K., Prigge, M., Schneider, F., Hegemann, P. & Gottschalk, A. Bimodal activation of different neuron classes with the spectrally red-shifted channelrhodopsin chimera C1V1 in Caenorhabditis elegans. *PloS one* **7**, e46827, doi:10.1371/journal.pone.0046827 (2012).

5 Stujenske, J. M., Spellman, T. & Gordon, J. A. Modeling the Spatiotemporal Dynamics of Light and Heat Propagation for In Vivo Optogenetics. *Cell reports* **12**, 525-534, doi:10.1016/j.celrep.2015.06.036 (2015).

6 Yizhar, O., Fenno, L. E., Davidson, T. J., Mogri, M. & Deisseroth, K. Optogenetics in neural systems. *Neuron* **71**, 9-34, doi:10.1016/j.neuron.2011.06.004 (2011).

7 Wietek, J. *et al.* Anion-conducting channelrhodopsins with tuned spectra and modified kinetics engineered for optogenetic manipulation of behavior. *Scientific reports* **7**, 14957, doi:10.1038/s41598-017-14330-y (2017).

8 Berndt, A. *et al.* Structural foundations of optogenetics: Determinants of channelrhodopsin ion selectivity. *Proc Natl Acad Sci U S A*, doi:10.1073/pnas.1523341113 (2015).

9 Govorunova, E. G., Sineshchekov, O. A., Janz, R., Liu, X. & Spudich, J. L. NEUROSCIENCE. Natural light-gated anion channels: A family of microbial rhodopsins for advanced optogenetics. *Science* **349**, 647-650, doi:10.1126/science.aaa7484 (2015).

10 Kleinlogel, S. *et al.* A gene-fusion strategy for stoichiometric and co-localized expression of light-gated membrane proteins. *Nat Methods* **8**, 1083-1088, doi:10.1038/nmeth.1766 (2011).

11 Gradinaru, V. *et al.* Molecular and cellular approaches for diversifying and extending optogenetics. *Cell* **141**, 154-165, doi:10.1016/j.cell.2010.02.037 (2010).

12 Lim, S. T., Antonucci, D. E., Scannevin, R. H. & Trimmer, J. S. A novel targeting signal for proximal clustering of the Kv2.1 K+ channel in hippocampal neurons. *Neuron* **25**, 385-397 (2000).

13 Hochbaum, D. R. *et al.* All-optical electrophysiology in mammalian neurons using engineered microbial rhodopsins. *Nat Methods* **11**, 825-833, doi:10.1038/nmeth.3000 (2014).

14 Breton-Provencher, V. & Sur, M. Active control of arousal by a locus coeruleus GABAergic circuit. *Nat Neurosci* **22**, 218-228, doi:10.1038/s41593-018-0305-z (2019).

15 Dimidschstein, J. *et al.* A viral strategy for targeting and manipulating interneurons across vertebrate species. *Nat Neurosci* **19**, 1743-1749, doi:10.1038/nn.4430 (2016).

16 Douin, V. *et al.* Use and comparison of different internal ribosomal entry sites (IRES) in tricistronic retroviral vectors. *BMC Biotechnol* **4**, 16, doi:10.1186/1472-6750-4-16 (2004).

17 Tang, W. *et al.* Faithful expression of multiple proteins via 2A-peptide self-processing: a versatile and reliable method for manipulating brain circuits. *J Neurosci* **29**, 8621-8629, doi:10.1523/JNEUROSCI.0359-09.2009 (2009).

18 Lima, S. Q., Hromadka, T., Znamenskiy, P. & Zador, A. M. PINP: a new method of tagging neuronal populations for identification during in vivo electrophysiological recording. *PloS one* **4**, e6099, doi:10.1371/journal.pone.0006099 (2009).

19 Ramirez, S. *et al.* Creating a false memory in the hippocampus. *Science* **341**, 387-391, doi:10.1126/science.1239073 (2013).